

# Chapter 3

## Multi-IRS-Assisted System With Switched Diversity

In this Chapter, the OP analysis of multiple IRS-assisted SISO systems with switched diversity schemes is presented. OP expressions for the dual-IRS-panel-aided SSC system and multiple-IRS-panel-aided SEC system are analyzed over Rician fading channels. Tight approximate OP expressions in closed form are derived for a large number of IRS elements, along with a simple asymptotic OP to study diversity order and coding gain.

### 3.1 Introduction

IRS-assisted wireless network is a key enabling technology for next-generation wireless networks. Recently it is a very popular research topic among the wireless research community. By smartly tuning the phase of the reflected signals, IRS is

capable of redirecting the electromagnetic signals dynamically in the desired direction [56, 57, 80]. IRS reconfigures wireless channel and it can improve the received signal strength by passive beamforming at the IRS panel. Therefore, the IRS panel improves the energy efficiency of the wireless system with high coverage area and low latency. It can also mitigate the deep fading scenario by suitably reconfiguring a wireless environment [60, 81]. In addition, IRS panel's hardware cost and complexity are lower as compared to conventional relaying systems [82]. Since IRS panels do not require RF chains.

The idea of IRS was proposed in [83, 84]. After this, IRS-assisted wireless communications have been extensively studied in the literature [30, 32, 65, 68, 85–90]. In [85], authors have studied about maximization of sum-rate of IRS-assisted multiuser system based on MISO configuration using deep reinforcement learning. Joint active and passive beamforming optimization to minimize the transmit power for an IRS-aided wireless network has been analyzed in [86]. For IRS assisted wireless network, a simplified path loss model has been derived in [32].

An IRS-based downlink multigroup multicast communication system is optimized to maximize the sum-rate for the power and unit-modulus constraints [87]. In [88], authors investigate a wireless network assisted by IRS with discrete phase shifts in terms of a beamforming optimization problem. In [30], an IRS-aided downlink multiuser communication scenario is studied for energy-efficient designs. The ergodic spectral efficiency of an IRS-based wireless communication system is investigated for Rician fading channels in [64]. Authors investigate achievable multicast rate for an IRS-based multi-antenna multicast system in [65]. In [31], authors study the achievable sum-rate performance of IRS-aided multiple-input multiple-output (MIMO)-based communication system. Basar et al., [32] present analytical performance limits of IRS-assisted communication systems over Rayleigh fading channels.

The coverage probability of an IRS-assisted wireless network is studied using stochastic geometry in [66]. The OP of IRS-assisted MISO system for the Rician fading channel using maximum ratio transmission is derived in [67]. In [68], an IRS-based downlink communication system is studied where the average sum-rate and ergodic capacity are obtained.

In [69], the OP, ASER, and achievable capacity rate bounds for IRS-aided SISO system are presented in Rayleigh fading channels. In [70], the OP and achievable capacity rate for IRS-aided SISO system are derived in generalized fading channels. In [35], an upper bound expression for the Shannon capacity, and an approximate expression for the OP are presented for the IRS-aided SISO systems over Rician fading channels. Yildirim et al, [71] have suggested various multiple IRS-assisted 6G wireless networks to achieve future requirements. The OP and asymptotic sum-rate are studied for multiple IRS-assisted networks over Rayleigh fading channels in [72]. In [89, 91], the impact of imperfect phase compensation is analyzed for IRS-aided multi-layer unmanned aerial vehicle (UAV) communications. The capacity of IRS-assisted UAV communication system with imperfect phase compensation is analyzed in [90]. An IRS-assisted network is analyzed for different communication scenarios in the literature.

In wireless communications, diversity means superiority. With the increase in the diversity order, the performance of wireless communication enhances. Explosive growth of heterogeneous networks due to the IoT and the internet of everything (IoE), there is huge demand of low complex and low-cost system design for next-generation wireless communications. To the best of the authors' knowledge, the OP performance of multiple IRS-assisted SISO wireless communication system with SSC and SEC diversities at IRS panels are not explored for independent and identically distributed (i.i.d.) Rician fading channels. We found this problem worthy for

exploration due to the simplicity of switched diversity and the popularity of IRS.

**Contributions:** In this chapter, multiple IRS-assisted wireless communication scenario is considered. We investigate the performance of IRS-assisted SISO system for dual-IRS-panels-aided SSC and multiple-IRS-panels-aided SEC diversities over i.i.d. Rician fading channels. The tight closed-form approximate OP expressions for dual-IRS-panel-aided SSC diversity and multiple-IRS-panels-aided SSE diversity systems are derived. In addition, we also derive a simple asymptotic OP of both SSC and SEC-based SISO system to get diversity order and coding gain. The impact of each system parameter such as distance, number of reflecting surfaces, threshold, fading parameter, etc. on the OP performance is thoroughly investigated. Further, multiple IRS panels significantly enhance system performance using a large number of reflecting elements in each IRS panel. These derived analytical expressions prove instrumental in evaluating the performance of future wireless networks aided by multiple IRS setups.

The rest of the chapter is structured as follows. Section 3.2 presents both system and channel models. The OP expressions are derived in Section 3.3. The simulation and numerical results are discussed in Section 3.4. Finally, Section 3.5 summarizes the chapter.

## 3.2 System and Channel Models

We have considered a SISO-based wireless communication system model in which Tx and Rx nodes have a single antenna. A direct link between Tx and Rx nodes is blocked due to severe path-loss or dense urban environment<sup>1</sup>. Rx is assisted by  $M$

---

<sup>1</sup>Or the direct link has very insignificant power.

IRS panels each having  $N_m$  reflecting elements, where  $1 \leq m \leq M$ , as shown in Figure 3.1. The IRS panels are connected to the IRS controller for switching operations. At a particular time instant, only one IRS panel will redirect the electromagnetic signals towards the Rx node using beamforming with perfect CSI.

The  $m$ -th received signal from  $m$ -th IRS panel to the receiving antenna can be expressed as [32]

$$r_m = \sqrt{P} (\mathbf{g}_m^T \mathbf{\Theta}_m \mathbf{h}_m) x_t + n_m, \quad 1 \leq m \leq M \quad (3.1)$$

where  $x_t$  is the transmitted message with unit energy,  $P$  is the transmit power of message  $x_t$ ,  $\mathbf{h}_m = [h_{m1}, h_{m2}, \dots, h_{mN_m}]$  and  $\mathbf{g}_m = [g_{m1}, g_{m2}, \dots, g_{mN_m}]$  are the vectors of channel coefficients between the Tx node to the  $m$ th IRS panel and the  $m$ th IRS panel to the receiving antenna of Rx node, respectively.  $\mathbf{\Theta}_m = \text{diag}\{[e^{j\theta_{m1}}, e^{j\theta_{m2}}, \dots, e^{j\theta_{mN_m}}]\}$  is a diagonal matrix, which consists of the phase shift values applied by the reflecting elements of the  $m$ th IRS panel, and  $n_m$  denotes the additive white Gaussian noise with zero mean and variance  $N_0$  at the receiving antenna. Since IRS panels are located at the LoS to both Tx node and Rx node. Thus,  $h_{mi}, 1 \leq i \leq N_m$  are modeled by Rician distribution with identical the Rician parameters  $K_{h_m}$ . Therefore, the channel coefficients between the Tx node and  $m$ th IRS panel can be written as [35]

$$h_{mi} = \frac{1}{\sqrt{d_{h_m}^{\alpha_{h_m}}}} \left( \sqrt{\frac{K_{h_m}}{K_{h_m} + 1}} \tilde{h}_{mi} + \sqrt{\frac{1}{K_{h_m} + 1}} \hat{h}_{mi} \right), \quad 1 \leq m \leq M \text{ and } 1 \leq i \leq N_m \quad (3.2)$$

where  $\alpha_{h_m}$  and  $d_{h_m}$  denote the path loss exponent and distance for the  $i$ -th channel between the Tx node and the corresponding  $m$ -th IRS, respectively. Also,  $\tilde{h}_{mi}$  and

and  $\hat{h}_{mi}$  are the normalized LoS component and the normalized NLoS component for the  $i$ -th channel between the Tx node and the corresponding  $m$ th IRS, respectively. Similarly,  $\mathbf{g}_{mi}, 1 \leq i \leq N_m$  are modeled by Rician distribution with identical the Rician parameter  $K_{g_m}$ , the channel coefficients between  $m$ th IRS panel and the receiving antenna can be written as [35]

$$\mathbf{g}_{mi} = \frac{1}{\sqrt{d_{g_m}^{\alpha_{g_m}}}} \left( \sqrt{\frac{K_{g_m}}{K_{g_m} + 1}} \tilde{\mathbf{g}}_{mi} + \sqrt{\frac{1}{K_{g_m} + 1}} \hat{\mathbf{g}}_{mi} \right), \quad 1 \leq m \leq M \text{ and } 1 \leq i \leq N_m \quad (3.3)$$

where  $d_{g_m}$  and  $\alpha_{g_m}$  denote the distance and path loss exponent for the  $i$ -th channel between the  $m$ th IRS and the receiving antenna, respectively. Also,  $\tilde{\mathbf{g}}_{mi}$  and  $\hat{\mathbf{g}}_{mi}$  are the normalized LoS component and the normalized NLoS component for the  $i$ th channel between the  $m$ th IRS and the receiving antenna, respectively.

Assuming that the channel phases are available to the IRS panel, applying the optimal co-phasing matrix  $\mathbf{\Theta}_m$ , the instantaneous optimal SNR  $\gamma_m$  of the  $m$ th received signal can be expressed as [32]

$$\gamma_m = \gamma_0 \left( \sum_{i=1}^{N_m} |h_{mi}| |\mathbf{g}_{mi}| \right)^2, \quad (3.4)$$

where  $\gamma_0 = \frac{P}{N_0}$  represents the transmit SNR. The IRS panel switching is assumed to be done at the discrete instant of time  $t = nT$ , where  $T$  is usually in the order of channel coherent time.  $\gamma_m(n)$  is the received signal power at the receiving antenna at time instant  $n$  after applying the switched diversity. If the  $m$ th IRS panel is used for transmission then  $\gamma(n) = \gamma_m(n)$ . We also assume that the successive sample received at the receiver from each IRS panel are independent.  $\gamma(n)$  selects according to SSC or SEC scheme as follows.

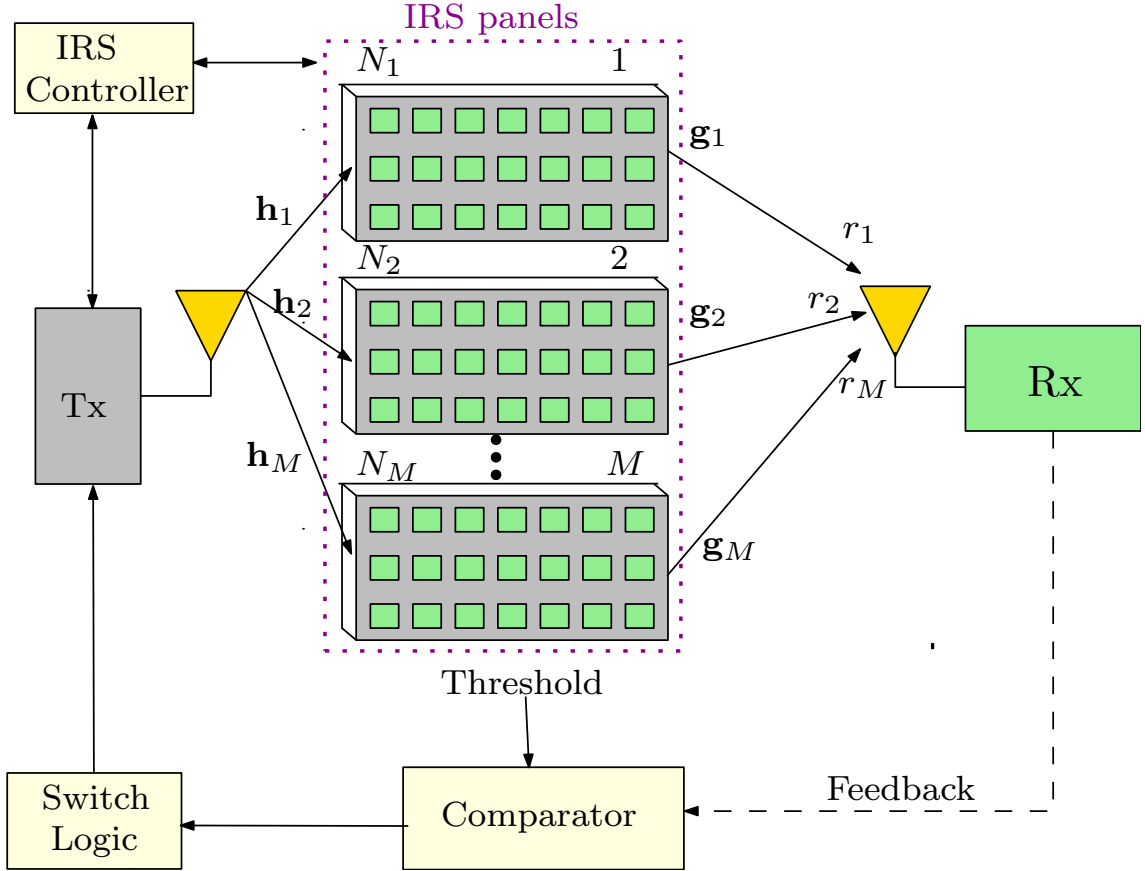


FIGURE 3.1: Multiple IRS-aided SISO communication system with switched diversity schemes.

### 3.2.1 Switching Operation for SSC Scheme

When the received signal power from the selected IRS panel goes below a predetermined threshold then the received signal branch becomes undesirable and an IRS panel switching is required. For SSC, the IRS panel switched to the next IRS panel branch whatever is the channel condition of the switched IRS panel. Thus, for the mentioned setup, the SSC operation can be written mathematically by the sequence  $\gamma(n)$  as given in (3.5), where  $((m-1)_M)$  denotes the  $m-1$  modulo  $M$ .

$$\gamma(n) = \gamma_m(n) \text{ iff } \begin{cases} \gamma(n-1) = \gamma_m(n-1), & \text{and } \gamma_m(n) \geq s_{th} \\ \text{or} \\ \gamma(n-1) = \gamma_{((m-1)_M)}(n-1), & \text{and } \gamma_{((m-1)_M)}(n) < s_{th} \end{cases} \quad (3.5)$$


---

### 3.2.2 Switching Operation for SEC Scheme

For SEC, the received signal power from the switched IRS panel is examined at the receiver, and the IRS panel switching occurs again if the received signal is impermissible. The receiver does this process again until either it finds a permissible IRS panel or a signal from all IRS panels has been examined. In the latter case, the previous examined IRS panel is used or switches back to the first IRS panel for the next transmission time slot. Both IRS selections lead to the same system performance.

Hence, the SEC operation can be written mathematically as given in (3.6) as,

$$\gamma(n) = \gamma_m(n) \text{ iff } \left\{ \begin{array}{l}
 \gamma(n-1) = \gamma_m(n-1), \quad \text{and } \gamma_m(n) \geq s_{th} \\
 \text{or} \\
 \gamma(n-1) = \gamma_m(n-1), \quad \text{and } \gamma_j(n) < s_{th}, j = 1, 2, \dots, M \\
 \text{or} \\
 \gamma(n-1) = \gamma_{((m-1)_M)}(n-1) \quad \text{and} \\
 \gamma_{((m-1)_M)}(n) < s_{th} \quad \text{and } \gamma_m(n) \leq s_{th} \\
 \vdots \\
 \text{or} \\
 \gamma(n-1) = \gamma_{((m-l)_M)}(n-1), \quad \text{and } \gamma_{((m-l+j)_M)}(n) < s_{th} \text{ and} \\
 \gamma_m(n) \geq s_{th}, j = 1, 2, \dots, l \\
 \vdots \\
 \text{or} \\
 \gamma(n-1) = \gamma_{((m-l)_M)}(n-1), \quad \text{and } \gamma_{((m-1+j)_M)}(n) < s_{th} \text{ and} \\
 \gamma_m(n) \geq s_{th}, j = 1, 2, \dots, M-1,
 \end{array} \right. \tag{3.6}$$

where  $m = 1, 2, 3, \dots, M$ .

### 3.3 Outage Probability Analysis

In this section, we have derived the approximate OP, the asymptotic OP, and the diversity order and the coding gain of the considered SIMO system with dual branch SSC over i.i.d. Rician channels.

### 3.3.1 Exact Outage Probability Expression for SSC Scheme

The OP of a dual-IRS-panel-aided SISO communication system with an SSC scheme can be expressed as

$$P_{\text{out}_{SSC}} = \begin{cases} F_{\gamma_m}(s_{th}) F_{\gamma_m}(\gamma_{th}), & \text{if } \gamma_{th} < s_{th} \\ F_{\gamma_m}(\gamma_{th}) - F_{\gamma_m}(s_{th}) + F_{\gamma_m}(\gamma_{th}) F_{\gamma_m}(s_{th}), & \text{otherwise} \end{cases} \quad (3.7)$$

where  $F_{\gamma_m}(\cdot)$  denotes the CDF of instantaneous SNR  $\gamma_m$ , and  $\gamma_{th}$  is a predefined threshold SNR, and  $s_{th}$  is a predefined fixed threshold SNR. Thus, one needs to derive an expression of  $F_{\gamma_m}(\cdot)$  to obtain the OP expression. It is also a well-known fact that the addition of a branch after two can not improve the performance of SSC scheme for the i.i.d. case.

### 3.3.2 Exact Outage Probability Expression for SEC Scheme

It is known that the addition of IRS panels after two can not improve the performance of SSC system. Therefore, the performance can be further enhanced by SEC diversity system by the addition of IRS panels of more than two. The OP of multiple-IRS-panel-aided SISO communication system using SEC scheme at IRS panels can be expressed as [8]

$$P_{\text{out}_{SEC}} = \begin{cases} (F_{\gamma_m}(s_{th}))^{M-1} F_{\gamma_m}(\gamma_{th}), & \text{if } \gamma_{th} < s_{th} \\ \sum_{j=1}^M (F_{\gamma_m}(\gamma_{th}) - F_{\gamma_m}(s_{th})) (F_{\gamma_m}(s_{th}))^j + (F_{\gamma_m}(s_{th}))^M, & \text{otherwise} \end{cases} \quad (3.8)$$

### 3.3.3 Effect of Branch Unbalance on Exact Outage Probability of SSC Scheme

Consider any pair ( $m = 1, 2$ ) of IRS panels, under an independent but not necessarily identically distributed SSC system. We can express the OP of this system as given [8].

$$P_{\text{out}_{SSC}} = \begin{cases} A(s_{th}) F_{\gamma_1}(s_{th}) (F_{\gamma_1}(\gamma_{th}) + F_{\gamma_2}(\gamma_{th})), & \text{if } \gamma_{th} < s_{th} \\ (1 - A(s_{th})) F_{\gamma_2}(\gamma_{th}) + A(s_{th}) F_{\gamma_1}(\gamma_{th}) (F_{\gamma_1}(\gamma_{th}) + F_{\gamma_2}(\gamma_{th}) - 2), & \text{otherwise,} \end{cases}$$

where  $A(s_{th}) = \frac{F_{\gamma_2}(s_{th})}{F_{\gamma_1}(s_{th}) + F_{\gamma_2}(s_{th})}$ .

### 3.3.4 Approximate OP Expressions for SSC and SEC Schemes

To compute each OP expression, one needs a tractable expression of  $F_{\gamma_m}(\cdot)$ . To the best of the authors' knowledge, it is not possible to derive an exact tractable expression for  $F_{\gamma_m}(\cdot)$  in closed-form. However, for a sufficiently large number of reflecting surfaces, i.e.,  $N_m \gg 1$ , with the aid of the central limit theorem, one can obtain an accurate approximate tractable closed-form expression for  $F_{\gamma_m}(\cdot)$ .

The instantaneous SNR of the  $m$ -th received signal can be expressed as

$$\gamma_m = \mathcal{A}_m^2 \gamma_0, \tag{3.9}$$

where  $\mathcal{A}_m = \sum_{i=1}^{N_m} |h_{mi}| |g_{mi}|$ . As we know that  $|h_{mi}|$  and  $|g_{mi}|$  are independent Rician distributed RVs. Now, for a sufficiently large number of reflecting surfaces, i.e.,  $N_m \gg 1$ , with the aid of the central limit theorem, the RV  $\mathcal{A}_m$  can model as

a normal distributed RV with the following mean  $\mu_m$  and variance  $\sigma_m^2$  [35]:

$$\mu_m = \frac{N_m \pi L_{0.5}(-K_{h_m}) L_{0.5}(-K_{g_m})}{4\sqrt{d_{h_m}^{\alpha_{h_m}} d_{g_m}^{\alpha_{g_m}} (K_{h_m} + 1) (K_{g_m} + 1)}}, \quad (3.10)$$

$$\sigma_m^2 = \frac{N_m}{d_{h_m}^{\alpha_{h_m}} d_{g_m}^{\alpha_{g_m}}} \left[ 1 - \frac{\pi^2 L_{0.5}^2(-K_{h_m}) L_{0.5}^2(-K_{g_m})}{16 (K_{h_m} + 1) (K_{g_m} + 1)} \right], \quad (3.11)$$

where  $L_m(\cdot)$  denotes the Laguerre polynomial of degree  $m$  [92]. Hence, the probability density function (PDF) of  $\mathcal{A}_m$  can be given by [9]

$$f_{\mathcal{A}_m}(x) = \frac{1}{\sqrt{2\pi\sigma_m^2}} \exp\left(-\frac{(x - \mu_m)^2}{2\sigma_m^2}\right). \quad (3.12)$$

The corresponding CDF of  $\mathcal{A}_m$  can be expressed as

$$\begin{aligned} F_{\mathcal{A}_m}(x) &= \Pr(\mathcal{A}_m \leq x) \\ &= \frac{1}{\sqrt{2\pi\sigma_m^2}} \int_{-\infty}^x \exp\left(-\frac{(t - \mu_m)^2}{2\sigma_m^2}\right) dt \\ &= 1 - Q\left(\frac{x - \mu_m}{\sigma_m}\right), \end{aligned} \quad (3.13)$$

where  $Q(\cdot)$  denotes the Gaussian  $Q$ -function [9]. Now, one can get the CDF of  $\gamma_m$  as the following

$$\begin{aligned} F_{\gamma_m}(x) &= \Pr(\gamma_m \leq x) = \Pr(\mathcal{A}_m^2 \gamma_0 \leq x) \\ &= 1 - Q\left(\frac{\sqrt{\frac{x}{\gamma_0}} - \mu_m}{\sigma_m}\right). \end{aligned} \quad (3.14)$$

Now, using (3.14) into (3.7), the OP of the dual-IRS-panel-assisted SISO wireless system with SSC diversity can be given by (3.15). Similarly, using (3.14) into (3.8),

the OP of the multiple-IRS-panel-assisted SISO wireless system with SEC diversity can be expressed by (3.16).

$$P_{\text{out}_{SSC}} = \begin{cases} \left(1 - Q\left(\frac{\sqrt{\frac{s_{th}}{\gamma_0}} - \mu_m}{\sigma_m}\right)\right) \left(1 - Q\left(\frac{\sqrt{\frac{\gamma_{th}}{\gamma_0}} - \mu_m}{\sigma_m}\right)\right), & \text{if } \gamma_{th} < s_{th} \\ \left(Q\left(\frac{\sqrt{\frac{s_{th}}{\gamma_0}} - \mu_m}{\sigma_m}\right) - Q\left(\frac{\sqrt{\frac{\gamma_{th}}{\gamma_0}} - \mu_m}{\sigma_m}\right)\right) + \left(1 - Q\left(\frac{\sqrt{\frac{s_{th}}{\gamma_0}} - \mu_m}{\sigma_m}\right)\right) \times \\ \left(1 - Q\left(\frac{\sqrt{\frac{\gamma_{th}}{\gamma_0}} - \mu_m}{\sigma_m}\right)\right), & \text{otherwise} \end{cases} \quad (3.15)$$

$$P_{\text{out}_{SEC}} = \begin{cases} \left(1 - Q\left(\frac{\sqrt{\frac{s_{th}}{\gamma_0}} - \mu_m}{\sigma_m}\right)\right)^{M-1} \left(1 - Q\left(\frac{\sqrt{\frac{\gamma_{th}}{\gamma_0}} - \mu_m}{\sigma_m}\right)\right), & \text{if } \gamma_{th} < s_{th} \\ \sum_{j=1}^M \left(Q\left(\frac{\sqrt{\frac{s_{th}}{\gamma_0}} - \mu_m}{\sigma_m}\right) - Q\left(\frac{\sqrt{\frac{\gamma_{th}}{\gamma_0}} - \mu_m}{\sigma_m}\right)\right) \left(1 - Q\left(\frac{\sqrt{\frac{s_{th}}{\gamma_0}} - \mu_m}{\sigma_m}\right)\right)^j + \\ \left(1 - Q\left(\frac{\sqrt{\frac{s_{th}}{\gamma_0}} - \mu_m}{\sigma_m}\right)\right)^M, & \text{otherwise} \end{cases} \quad (3.16)$$

### 3.3.5 Asymptotic OP Expression for SSC and SEC Schemes

The OP expressions are derived in (3.15) and (3.16) for the SSC and SEC schemes for all SNR scenarios. Moreover, to understand the effect of the number of IRS panels, OP expressions are derived at high SNR scenarios, and it is referred as asymptotic OP. To obtain the asymptotic OP expression, assuming each link is subjected to high SNR  $\bar{\gamma}_m = \mathbf{E}[\gamma_m] \rightarrow \infty$ , where  $\mathbf{E}[\cdot]$  is a statistical averaging operator. Using [78, (22)], an approximate asymptotic PDF expression of RV  $z_{mi} = |h_{mi}| |g_{mi}|$  can

be obtained as

$$f_{z_{mi}}^\infty(x) \approx 4\Delta d_{h_m}^{\alpha_{h_m}} d_{g_m}^{\alpha_{g_m}} (1 + K_{h_m}) (1 + K_{g_m}) x \exp(- (K_{h_m} + K_{g_m})). \quad (3.17)$$

Details of (3.17) are given in Appendix-A in Section B. Further, the corresponding asymptotic moment generating function (MGF) of RV  $z_{mi}$  can be given by

$$\begin{aligned} \mathcal{M}_{z_{mi}}^\infty(s) &= \int_0^\infty \exp(-s x) f_{z_{mi}}^\infty(x) dx \\ &= 4\Delta d_{h_m}^{\alpha_{h_m}} d_{g_m}^{\alpha_{g_m}} (1 + K_{h_m}) (1 + K_{g_m}) \exp(- (K_{h_m} + K_{g_m})) s^{-2}. \end{aligned} \quad (3.18)$$

Since,  $z_{mi}$  are i.i.d. RVs, the MGF expression of  $\mathcal{A}_m$  can be written as

$$\mathcal{M}_{\mathcal{A}_m}^\infty(s) = (\mathcal{M}_{z_{mi}}^\infty(s))^{N_m} = \lambda_m s^{-2N_m}, \quad (3.19)$$

where  $\lambda_m = (4\Delta d_{h_m}^{\alpha_{h_m}} d_{g_m}^{\alpha_{g_m}} (1 + K_{h_m}) (1 + K_{g_m}))^{N_m} \exp(-N_m (K_{h_m} + K_{g_m}))$ . Taking inverse Laplace transform of  $s^{-1} \mathcal{M}_{\mathcal{A}_m}^\infty(s)$ , one can obtain the CDF expression of  $\mathcal{A}_m$  as

$$F_{\mathcal{A}_m}^\infty(x) = \frac{\lambda_m x^{2N_m}}{\Gamma(2N_m + 1)}, \quad (3.20)$$

where  $\Gamma(\cdot)$  denotes the gamma function. Hence, one can get the CDF of  $\gamma_m$  as

$$F_{\gamma_m}^\infty(x) = \Pr(\gamma_m \leq x) = \Pr(\mathcal{A}_m^2 \gamma_0 \leq x) = \frac{\lambda_m x^{N_m}}{\Gamma(2N_m + 1) \gamma_0^{N_m}}. \quad (3.21)$$

Putting (3.21), into (3.7) the OP of the dual-IRS-panel-aided SISO wireless system with SSC diversity can be given as

$$P_{\text{out}_{SSC}}^{\infty} = \begin{cases} \frac{\lambda_{th}^{N_m} s_{th}^{N_m}}{\gamma_0^{2N_m}} \left( \frac{\lambda_m}{\Gamma(2N_m+1)} \right)^2, & \text{if } \gamma_{th} < s_{th} \\ \frac{\lambda_m(\lambda_{th}^{N_m} - s_{th}^{N_m})}{\Gamma(2N_m+1)\gamma_0^{N_m}} + \frac{\lambda_{th}^{N_m} s_{th}^{N_m}}{\gamma_0^{2N_m}} \left( \frac{\lambda_m}{\Gamma(2N_m+1)} \right)^2, & \text{otherwise} \end{cases} \quad (3.22)$$

Similarly, by substituting (3.21), into (3.8) the OP of the multiple-IRS-panel-aided SISO wireless system with SEC diversity is given by

$$P_{\text{out}_{SEC}}^{\infty} = \begin{cases} \frac{\lambda_{th}^{N_m} s_{th}^{N_m(M-1)}}{\gamma_0^{MN_m}} \left( \frac{\lambda_m}{\Gamma(2N_m+1)} \right)^M, & \text{if } \gamma_{th} < s_{th} \\ \sum_{j=1}^M \frac{\lambda_m(\lambda_{th}^{N_m} - s_{th}^{N_m})}{\Gamma(2N_m+1)\gamma_0^{N_m}} \left( \frac{\lambda_m(s_{th})^{N_m}}{\Gamma(2N_m+1)\gamma_0^{N_m}} \right)^j + \left( \frac{\lambda_m(s_{th})^{N_m}}{\Gamma(2N_m+1)\gamma_0^{N_m}} \right)^M, & \text{otherwise} \end{cases} \quad (3.23)$$

### 3.3.6 Diversiy Order and Coding Gain

In general, the asymptotic OP can be expressed as [13]

$$P_{\text{out}}^{\infty} = (\mathcal{G}_c \gamma_0)^{-\mathcal{G}_d}, \quad (3.24)$$

where  $\mathcal{G}_d$  and  $\mathcal{G}_c$  are the diversity order and the coding gain, respectively. It can be noticed from (3.22) that the  $G_d$  and  $G_c$  of the dual-IRS-panel-assisted SISO system with SSC scheme over Rician fading channel are  $\mathcal{G}_d = 2N_m$  and  $G_c = (\lambda_{th} s_{th})^{-\frac{1}{2}} \left( \frac{\lambda_m}{\Gamma(2N_m+1)} \right)^{-\frac{1}{N_m}}$ , if  $\gamma_{th} < s_{th}$ , respectively. Similarly, it can be also obtained from (3.23) that the  $G_d$  and  $G_c$  gain of the multiple-IRS-panel-assisted SISO system with SEC scheme over Rician fading channel are  $\mathcal{G}_d = MN_m$  and

$G_c = (\lambda_{th})^{-\frac{1}{M}} (s_{th})^{-\frac{M-1}{M}} \left( \frac{\lambda_m}{\Gamma(2N_m+1)} \right)^{-\frac{1}{N_m}}$ , if  $\gamma_{th} < s_{th}$ . The diversity gain of the IRS-assisted SISO system improves as the IRS panels increases. Therefore, the asymptotic OP reveals coding and diversity gains of SSC and SEC schemes clearly in (3.22) and (3.23) as compared to the exact OP expressions.

### 3.4 Numerical and Simulation Results

In this section, the derived OP expressions are numerically computed to analyze the IRS-assisted SISO communication system with SSC and SEC schemes. The Monte Carlo simulations are also presented to validate our derived OP expression. For convenient presentation, we assume the following assumption for parameters:  $K_{h_m} = K_1, K_{g_m} = K_2, d_{h_m} = d_1, d_{g_m} = d_2, \alpha_{h_m} = \alpha_1, \alpha_{g_m} = \alpha_2, \forall m$ . In addition, the following set of parameters are also taken for the numerical and the simulation results, unless it is stated exclusively. We select a sub-6G scenario, where the bandwidth of the system is 180 KHz, the power spectral density of the noise is  $-173$  dBm/Hz, the distances (in meter) are taken to be  $d_1 = d_2 = 150$  m, the path loss exponents are  $\alpha_1 = \alpha_2 = 2$ , the fading parameters are set to be  $K_1 = K_2 = K = 1$ , the reference path loss is  $-30$  dB at the reference distance  $d_0 = 1$  m, and the threshold SNR values are taken to be  $\gamma_{th} = 10$  dB and  $s_{th} = 12$  dB. In each figure, the OP performance is plotted against transmitted power  $P$  (dBm)<sup>2</sup> except Figure 3.8 and Figure 3.9.

Figure. 3.2 depicts the OP performance as a function of  $P$  for without diversity scheme ( $M = 1$ ), SSC scheme ( $M = 2$ ), and SEC scheme ( $M = 3, 4$ ) with different thresholds  $s_{th} = 12$  dB and  $\gamma_{th} = 10$  dB. The simulation results are matching closely

---

<sup>2</sup>SNR is expressed as  $P/N_0$ . Therefore, by keeping  $N_0$  constant and varying  $P$ , SNR changes in the system.

with the analytical results, as observed in Figure 3.2. One can notice that the OP performance improves sharply when either  $P$ , or  $M$  increases. The multiple IRS-assisted SISO system outperforms the single IRS-assisted SISO system with switched diversity schemes (SSC and SES). The OP performance of SEC diversity scheme is better than the SSC scheme, as expected due to multiple IRS. For example, at a fixed  $P_{\text{out}} = 10^{-3}$ , 0.4 dB of the transmit power gain is observed by varying  $M$  from 1 to 2. However, 1 dB of the transmit power gain is observed by increasing  $M = 1$  to  $M = 4$ .

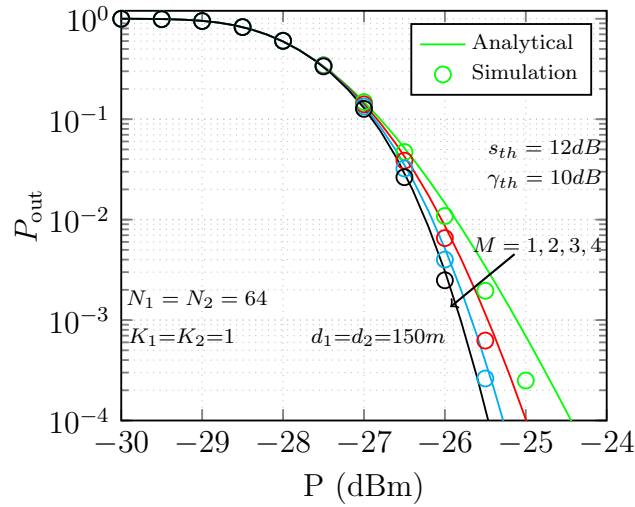


FIGURE 3.2: OP performance w.r.t  $P$  (dBm) for without diversity scheme ( $M = 1$ ), SSC scheme ( $M = 2$ ) and SEC scheme ( $M = 3, 4$ ).

Figure 3.3 shows the OP performance of SISO system without diversity scheme ( $M = 1$ ) and SSC and SEC diversity schemes ( $M = 2, 3, 4$ ) with identical threshold values  $s_{th} = \gamma_{th} = 10$  dB. It is important to recall here that when  $s_{th} = \gamma_{th}$ , the switched diversity schemes behave as a selection combining diversity scheme. From Figure 3.3, one can get similar observations to Figure 3.2. For example, at a fixed  $P_{\text{out}} = 10^{-3}$ , 1.2 dB of the transmit power gain is observed by varying  $M$  from 1 to 2 for a fixed  $N_m = 64$ . However, 2 dB of the transmit power gain is observed by increasing  $M = 1$  to  $M = 4$  for  $s_{th} = \gamma_{th} = 10$  dB, as observed in Figure 3.3.

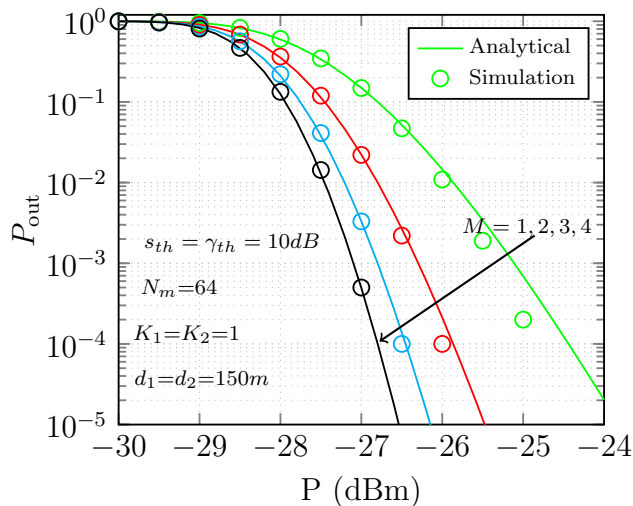


FIGURE 3.3: OP performance w.r.t  $P$  (dBm) for without diversity scheme ( $M = 1$ ) and switched diversity schemes ( $M = 2, 3, 4$ ).

Figure 3.4 and Figure 3.5 are presented to confirm the accuracy of derived asymptotic OP expressions at the high SNR region for both the SSC ( $M = 2$ ) and SEC ( $M = 4$ ) schemes, respectively. It can be observed that the asymptotic OP is approaching the exact OP at high transmit power, as shown in Figure 3.4 and Figure 3.5. Thus, it validates the accuracy of  $P_{\text{out}_{SSC}}^{\infty}$  and  $P_{\text{out}_{SEC}}^{\infty}$  expressions. Moreover, one can also observe from the slope of the OP curves at the high SNR region that the diversity order is equal to  $MN_m$ .

Figure 3.6 shows the OP performance as a function of the Rician factor  $K_{h_m} = K_{g_m} = K$  and  $P$ . The OP performance improves with an increase in  $K$  because the fading severity decrease with an increase in  $K$ . For example, at fixed  $P_{\text{out}} = 10^{-2}$ , a 2.5 dB of the transmit power gain is obtained when  $K$  increases from 0 to 10, as shown in Figure 3.6.

Figure 3.7 is presented to study the impact of  $N_m$  on the OP performance. OP is plotted by varying the transmitted power in Figure 3.7. We observe from Figure 3.7 that as  $N_m$  increases, the OP performance improves because the diversity order of the considered system model increases with an increase in  $N_m$ . For example, at fixed

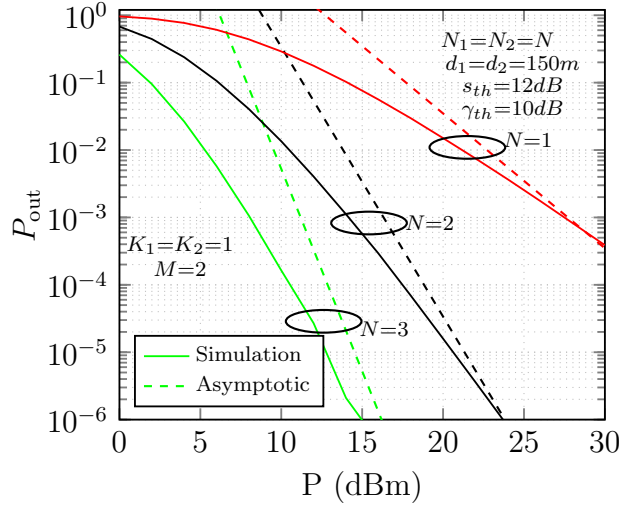


FIGURE 3.4: Asymptotic OP performance with varying the number of IRS elements  $N_m$  for SSC scheme.

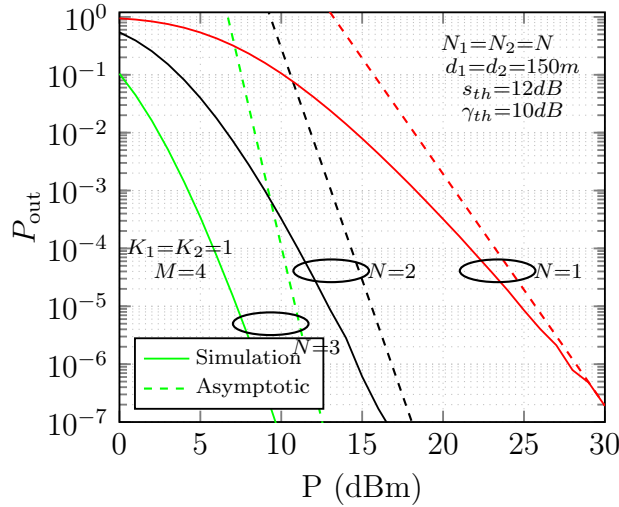


FIGURE 3.5: Asymptotic OP performance with varying the number of IRS elements  $N_m$  for SEC scheme.

$P_{\text{out}} = 10^{-3}$  by increasing  $N_m = 32$  to  $N_m = 128$ , we can observe the performance enhancement of around 2.5 dB in terms of transmit power, as depicted in Figure 3.7

Further, we analyze the impact of threshold  $\gamma_{th}$  in Figure 3.8 on the OP using both SSC and SEC schemes. It is observed that an increase in  $\gamma_{th}$  results in poor OP due to fixed transmit power. It is found that the SEC scheme outperforms the SSC

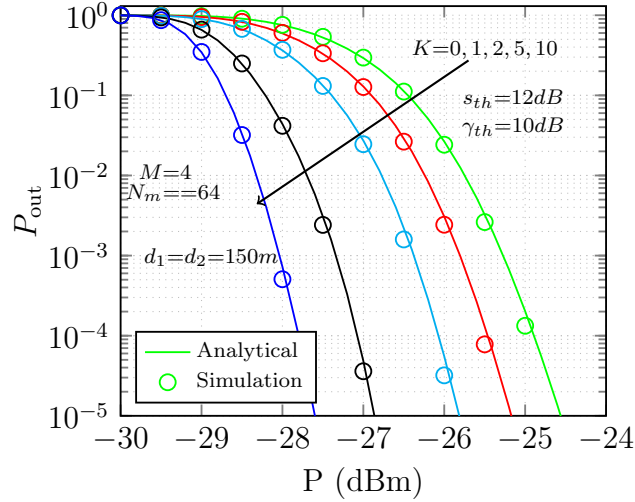


FIGURE 3.6: OP performance with varying the fading parameter  $K$  for SEC scheme.

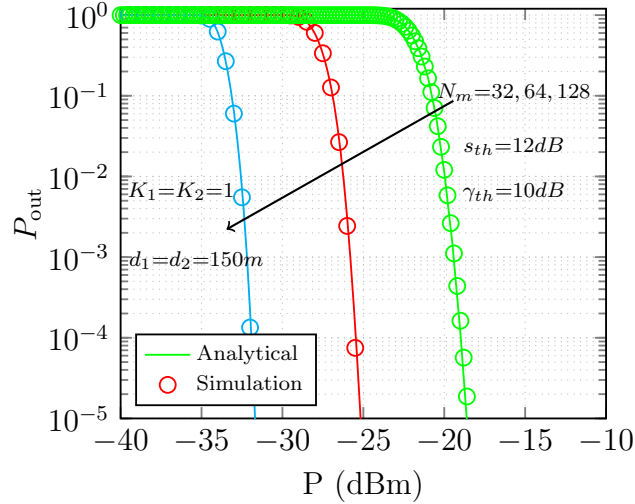


FIGURE 3.7: OP performance with varying the number of IRS elements in the panels  $N_m = 32, 64, 128$  and  $M = 4$  for SEC scheme.

scheme, as expected due to multiple IRS, as shown Figure 3.8. Further, it can be observed that shape of OP changes at  $\gamma_{th} = s_{th} = 12$  dB as expressed in theoretical results.

Next, Figure 3.9 illustrates the impact of distance  $d_1$  of IRS panels in between the Tx and Rx nodes on the OP performance with fixed  $d_1 + d_2 = 300m$ . It can be observed that the OP performance improves for the IRS panels placed closer to either the Tx

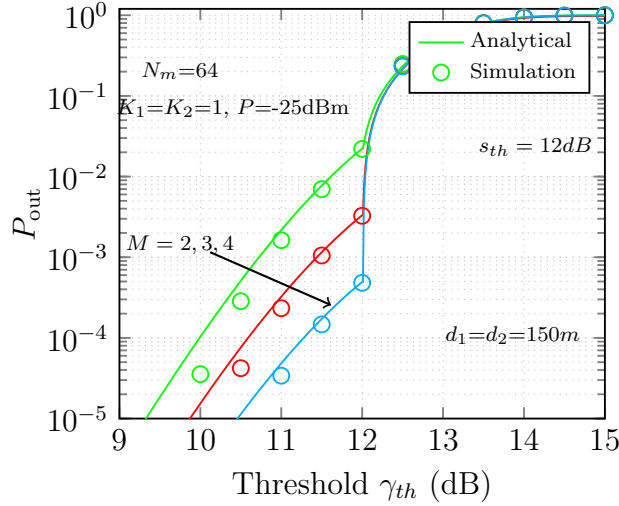


FIGURE 3.8: OP performance w.r.t threshold  $\gamma_{th}$  of SSC ( $M = 2$ ) and SEC ( $M = 3, 4$ ) schemes at fixed  $N_m = 64$ .

node or the Rx node. The reason is that the IRS panels placed closer to either the Tx node or the Rx node have small path loss. Thus, it can provide better signal strength. The OP performance is symmetric about the equidistant positions. For example if we compare equidistant IRS positions (150m) with the other positions, the OP performance is worst at equidistant positions due to higher path loss.

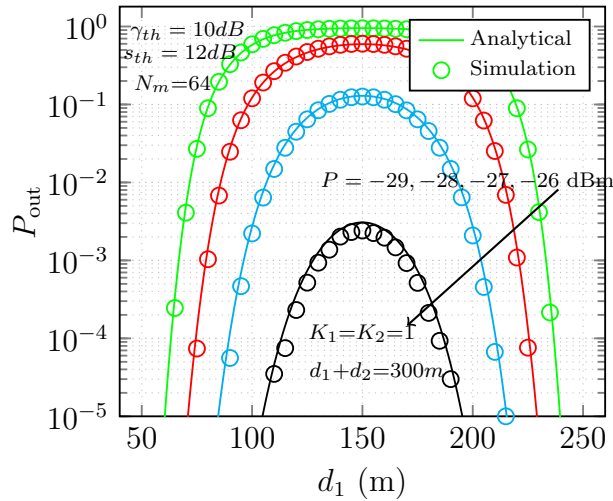


FIGURE 3.9: OP performance w.r.t distance  $d_1$  of SEC for  $M = 4$  and fixed  $N_m = 64$  for SEC.

### **3.5 Summary**

The performance of multiple-IRS-assisted SISO communication system with an SSC and SEC schemes has been comprehensively studied for Rician fading channels. An accurate OP expressions have been presented in closed-form for a large number of IRS elements. In addition, the asymptotic OP expressions have been also obtained which gives the diversity gain and the coding gain expressions. All obtained analytical expressions have been evaluated to demonstrate the system performance. The impact of the number of IRS elements, the number of IRS panels, the fading parameter, and the placement of IRS panels have been studied. Moreover, the Monte Carlo simulation results have been also given to confirm the accuracy of the presented theoretical analysis.